JPn Neuroscience

The Journal of Physiology

J Physiol 592.4 (2014) pp 795–809

Mechanisms by which a *CACNA1H* mutation in epilepsy patients increases seizure susceptibility

Veit-Simon Eckle[1], Aleksandr Shcheglovitov[1], Iuliia Vitko[1], Deblina Dey[1,2], Chan Choo Yap[3], Bettina Winckler[2,3] and Edward Perez-Reyes[1,3]

Departments of [1]Pharmacology and [2]Neuroscience, and [3]Neuroscience Graduate Program, University of Virginia School of Medicine, Charlottesville, VA, USA

Key points

- Mutations in the $Ca_v3.2$ T-type Ca^{2+} channel were found in patients with idiopathic generalized epilepsies, yet the mechanisms by which these mutations increase neuronal excitability and susceptibility to seizures remain to be determined.
- Using electrophysiological and transfection methods, we validate in cultured hippocampal neurons the hypothesis that an epilepsy mutation increases neuronal excitability.
- Mutations in the I–II loop of the channel increase trafficking to the plasma membrane without altering trafficking into dendrites. Mutations also enhance dendritic arborization.
- Additionally, we provide the first evidence that $Ca_v3.2$ can signal to Ca^{2+}-regulated transcription factors, which are known to play important roles in neuronal development and gene expression.

Abstract T-type calcium channels play essential roles in regulating neuronal excitability and network oscillations in the brain. Mutations in the gene encoding $Ca_v3.2$ T-type Ca^{2+} channels, *CACNA1H*, have been found in association with various forms of idiopathic generalized epilepsy. We and others have found that these mutations may influence neuronal excitability either by altering the biophysical properties of the channels or by increasing their surface expression. The goals of the present study were to investigate the excitability of neurons expressing $Ca_v3.2$ with the epilepsy mutation, C456S, and to elucidate the mechanisms by which it influences neuronal properties. We found that expression of the recombinant C456S channels substantially increased the excitability of cultured neurons by increasing the spontaneous firing rate and reducing the threshold for rebound burst firing. Additionally, we found that molecular determinants in the I–II loop (the region in which most childhood absence epilepsy-associated mutations are found) substantially increase the surface expression of T-channels but do not alter the relative distribution of channels into dendrites of cultured hippocampal neurons. Finally, we discovered that expression of C456S channels promoted dendritic growth and arborization. These effects were reversed to normal by either the absence epilepsy drug ethosuximide or a novel T-channel blocker, TTA-P2. As Ca^{2+}-regulated transcription factors also increase dendritic development, we tested a transactivator trap assay and found that the C456S variant can induce changes in gene transcription. Taken together, our findings suggest that gain-of-function mutations in $Ca_v3.2$ T-type Ca^{2+} channels increase seizure susceptibility by directly altering neuronal electrical properties and indirectly by changing gene expression.

V.-S. Eckle, A. Shcheglovitov and I. Vitko are co-first authors and contributed equally to the paper.

DOI: 10.1113/jphysiol.2013.264176

(Received 23 August 2013; accepted after revision 19 November 2013; first published online 25 November 2013)
Corresponding author E. Perez-Reyes: Jordan Hall 800735, 1340 Jefferson Park Avenue, Charlottesville, VA 22908, USA. Email: eperez@virginia.edu

Abbreviations ADP, after-depolarizing potential; AP, action potential; CAE, childhood absence epilepsy; DIV, days *in vitro*; EPSP, excitatory postsynaptic potential; ESX, ethosuximide; GFP, green fluorescent protein; HVA, high voltage-activated; IGE, idiopathic generalized epilepsy; IPSP, inhibitory postsynaptic potential; ISI, inter-spike interval; *I–V*, current voltage; LTS, low-threshold spike; LVA, low voltage-activated; PM, plasma membrane; SNP, single nucleotide polymorphism; TLE, temporal lobe epilepsy; V_m, resting membrane potential; UTR, untranslated region; WT, wild-type

Introduction

The entry of Ca^{2+} ions through T-channels leads to depolarization of the membrane, allowing T-currents to generate low-threshold spikes (LTSs) that trigger bursts of Na^+-dependent action potentials (APs) (Llinás, 1988). This role is especially prominent in thalamic neurons, which express T-currents at very high densities (Perez-Reyes, 2003; Cheong & Shin 2013). Thalamic neurons form a reciprocally connected circuit that oscillates during natural processes like sleep, but can also oscillate at inappropriate times such as during a seizure (McCormick & Contreras 2001). This circuit is composed of thalamic reticular nucleus neurons (GABAergic), thalamocortical neurons that reside in the relay nuclei (glutamatergic), and cerebral cortical neurons (glutamatergic).

The unique voltage dependence of T-channel gating also allows them to enhance neuronal firing after either an inhibitory or excitatory postsynaptic potential (IPSP, EPSP) (Crunelli & Leresche 2002; Cheong & Shin 2013). Such rebound burst firing occurs because T-channels are inactivated at the resting membrane potential of many neurons, and recover from inactivation during an IPSP. As the IPSP decays and the resting membrane potential is restored, T-channels can open and create an LTS.

Another very interesting property of T-channels is their ability to generate window currents. Window currents arise when a channel is available to open at a given potential and not totally inactivated; they are operationally defined by the overlap region between the steady-state activation and inactivation curves. Notably, T-window currents occur at the resting membrane potential of most neurons, allowing them to contribute to membrane bistability; for example, thalamic neurons have two 'resting' membrane potentials, one around −77 mV, and a second around −60 mV (Crunelli *et al.* 2005). $Ca_v3.2$ channels have been shown to generate window currents and increase resting basal Ca^{2+} concentrations (Chemin *et al.* 2000). A defining property of low voltage-activated (LVA) T-channels is that they open after small depolarizations from the resting membrane potential, at which there is a large driving force for Ca^{2+} entry. Their opening can lead to robust increases in intracellular Ca^{2+}, especially in small compartments such as dendrites and synaptic terminals (Munsch *et al.* 1997; Zhou *et al.* 1997; Huang *et al.* 2011).

Considerable evidence supports the hypothesis that T-channels play roles in epilepsy and pain (Nelson *et al.* 2006). In particular, T-channels are thought to play an important role in idiopathic generalized epilepsies (IGEs) such as absence epilepsy as a result of their high expression in the thalamus. Among the first targets identified for absence seizure drugs were T-channels (Coulter *et al.* 1989). Drugs that are useful in treating absence epilepsy, such as ethosuximide, are capable of blocking native rat T-currents at therapeutically relevant concentrations (Coulter *et al.* 1989), a finding supported by studies with recombinant human channels (Gomora *et al.* 2001). In addition to being supported by pharmacology studies, this hypothesis is further backed by studies in the GAERS (genetic absence epilepsy rat from Strasbourg) model of absence epilepsy. Reticular thalamic neurons isolated from these rats have 55% larger T-currents than the control strain and show a 16% increase in $Ca_v3.2$ mRNA (Tsakiridou *et al.* 1995; Talley *et al.* 2000). Similar results were found in the WAG/Rij model of absence epilepsy (Broicher *et al.* 2008).

Monogenic disorders in ion channels are relatively rare and typically lead to profound changes in gating. In contrast, IGEs are polygenic disorders (Gargus, 2003). The first evidence for this mode of inheritance came from Dr Lennox's study of epilepsy in twins (Vadlamudi *et al.* 2004). Other characteristics of polygenic disorders found in absence epilepsy include a variable age of onset, a variable age of recovery, and periodicity (Gargus, 2003). Furthermore, generalized spike-and-wave discharges were observed in family members without a history of seizures (Sander, 1996). Finally, the conclusion from many linkage studies is that the complex pattern of IGE inheritance is not attributable to a single gene, but that 'each gene contributes a small or modest effect to the epilepsy phenotype, and by itself is insufficient to cause epilepsy. These are "susceptibility genes"' (Tan *et al.* 2004). Therefore, common single nucleotide polymorphisms (SNPs) can contribute to epilepsy susceptibility. More importantly, a number of SNPs have been found only in epilepsy patients. The first of these studies was performed in childhood absence epilepsy (CAE) patients, leading to the

identification of 12 specific variants in the $Ca_v3.2$ gene, *CACNA1H*, associated with CAE (Chen *et al.* 2003). Interestingly, patients from three separate families harboured both the G773D variant and the 'common' SNP R788C, which was found in 20% of CAE patients and 10% of the general population (Vitko *et al.* 2005). Subsequent studies extended the finding of *CACNA1H* variants to many related epilepsies, such as juvenile absence epilepsy, juvenile myoclonic epilepsy, febrile seizures and temporal lobe epilepsy (TLE) (Heron *et al.* 2007; Klassen *et al.* 2011).

The present study investigates how *CACNA1H* variants increase seizure susceptibility. Studies on the initial CAE variants suggested that the majority caused changes in the biophysical properties of the channel (Vitko *et al.* 2005). Computer modelling was used to predict the net sum of these changes on neuronal firing and suggested that many, but not all, variants may increase seizure susceptibility by increasing T-channel opening. Subsequent studies showed all of the CAE variants located in the I–II loop increased surface expression, thereby providing a unifying mechanism for their role in seizure susceptibility (Vitko *et al.* 2007). All these studies were performed using transient transfection of HEK-293 cells. The present study extends these findings to cultured hippocampal neurons and validates the hypothesis that epilepsy mutations induce hyperexcitability of neurons. The study also implicates the role of endoplasmic reticulum trafficking motifs as a target of channel mutations. Using the transactivator trap assay developed by Ghosh and co-workers (Aizawa *et al.* 2004), we provide the first evidence that $Ca_v3.2$ can signal to Ca^{2+}-regulated transcription factors, which are known to play important roles in neuronal development and gene expression (West & Greenberg 2011). We conclude that mutations in $Ca_v3.2$ can increase seizure susceptibility by a variety of mechanisms, and that altering gene expression increases the probability that a mutation in a second gene might tip the balance towards seizure susceptibility.

Methods

Ethical approval

Experiments were carried out in accordance with institutional and federal guidelines, including those of the National Institutes of Health Guide for the Care and Use of Laboratory Animals (NIH Publication No. 8023, revised 2002). Rats were housed in a local animal facility in accordance with protocols approved by the University of Virginia Animal Use and Care Committee.

Transfection of cultured hippocampal neurons

Hippocampal neurons were prepared from embryonic day 18 (E18) Sprague–Dawley rats. Hippocampi were dissected, dissociated by trituration after trypsin digestion, and plated on poly-L-lysine-coated coverslips (Sigma-Aldrich Corp., St Louis, MO, USA). Cells were plated into Dulbecco's modified Eagle's medium (DMEM) supplemented with Glutamax (Life Technologies, Inc., Carlsbad, CA, USA), 10% horse serum, 1% sodium pyruvate and 1% penicillin G/streptomycin (plating medium). After 4 h, the medium was exchanged for conditioned serum-free medium supplemented with 2% B-27 (Life Technologies, Inc.) and 1% L-glutamine (growth medium). For electrophysiology and trafficking experiments, cultures were transfected at 7–8 days *in vitro* (DIV). Neurons were transfected with 1 μg of plasmids carrying appropriate channel variants using Lipofectamine 2000 (Life Technologies, Inc.). After 1 h of incubation, the medium was exchanged for growth medium. Cultures were maintained at 37°C for 4–6 days prior to electrophysiological experiments. For experiments measuring the growth of neurons, cells were transfected at 1 DIV with Lipofectamine 2000.

Plasmids

Human $Ca_v3.2a$ cDNA (GenBank accession no. AF051946) was used as $Ca_v3.2$ wild-type (WT) and mutated using single-overlap extension or QuikChange (Stratagene, Agilent Technologies, Inc., La Jolla, CA, USA) techniques as described previously (Vitko *et al.* 2005). Electrophysiology studies used a novel bicistronic vector in which the channel cDNA was followed by IRES-2 (Clontech Laboratories, Inc., Mountain View, CA, USA) and mCherry. Trafficking studies used a modified version of pcDNA in which expression is driven by the human synapsin-1 promoter. The plasmid expresses both green fluorescent protein (GFP) and the T-channel cDNA separated by a 2A peptide bridge (Tang *et al.* 2009). Plasmid maps are presented in Supplemental Fig. 1.

Electrophysiology

Coverslips containing transfected cells were placed in a recording chamber (RC-26G; Warner Instruments LLC, Hamden, CT, USA). The extracellular recording solution contained 140 mM NaCl, 5.4 mM KCl, 1.8 mM $CaCl_2$, 0.6 mM $MgCl_2$, 0.6 mM NaH_2PO_4, 1 mM $NaHCO_3$, 5.5 mM glucose and 10 mM Hepes, adjusted to pH 7.4. The intracellular solution for voltage-clamp recordings contained 135 mM tetramethylammonium, 10 mM EGTA, 14 mM Na_2HPO_4 and 10 mM Hepes, adjusted to pH 7.2 with hydrofluoric acid (Nelson *et al.* 2005). The intracellular solution for current-clamp recordings contained 120 mM potassium D-gluconate, 20 mM KCl, 4 mM MgATP, 0.3 mM NaGTP, 0.2 mM EGTA, 14 mM Na_2HPO_4 and 10 mM Hepes, adjusted to pH 7.2. Recording pipettes were

pulled from thin wall borosilicate glass (G150T-3; Warner Instruments LLC) to a final tip resistance of 3–5 MΩ for hippocampal neurons. Transfected cells were visualized by fluorescence microscopy with oblique illumination (BX50WI microscope; Olympus Corp., Tokyo, Japan). To isolate intrinsic activity of transfected neurons, the following blockers of synaptic transmission were added to the external solution: 2-amino-5-phosphonovaleric acid (30 μM); 6-cyno-7-nitroquinoxaline-2, 3-dione disodium salt (10 μM); saclofen (30 μM), and bicuculline methiodide (20 μM). Currents were recorded using a Multiclamp 700B amplifier, computer (Dell, Inc., Round Rock, TX, USA), Digidata 1322A A/D converter, and Clampex 9.2 software (Molecular Devices, LLC, Sunnyvale, CA, USA). Series resistance and cell capacitance were compensated to the maximal possible extent. In hippocampal neurons access resistance and cell capacitance were typically 12.6 ± 1.5 MΩ (n = 14) and 107 ± 20 pF (n = 14), respectively. All recordings were performed at room temperature. The loose cell-attached patch recording configuration (Nunemaker *et al.* 2003) was used to characterize spontaneous firing of neurons without disturbing the intracellular milieu.

Measuring trafficking of $Ca_v3.2$ and variants

Mature (7–8 DIV) hippocampal neurons were transfected with a single plasmid encoding both HA-tagged $Ca_v3.2$ channels and GFP. The signal from GFP was used to visualize the entire neuron. To localize channels at the plasma membrane (PM), live neurons were stained using a monoclonal anti-HA primary antibody (1 : 100 dilution, clone 16B12; Covance, Inc., Princeton, NJ, USA) for 30 min at 37°C. Cells were then fixed with 4% paraformaldehyde plus 4% sucrose for 15 min. Cells were washed three times with phosphate-buffered saline and then stained with a goat anti-mouse IgG secondary antibody coupled to Alexa Fluor 568 (1 : 400 dilution; Life Technologies, Inc.) for 60 min at room temperature. Cells were mounted with ProLong Gold antifade reagent (Life Technologies, Inc.). Images were collected on an Olympus BX61WI microscope equipped with appropriate fluorescent filter sets, various objectives (10×, 40×), and a Sensicam QE camera (Cooke Corp., Auburn Hills, MI, USA). IPLab 4.0 (Spectra Services, Inc., Ontario, NY, USA) was used for acquisition and analysis. Neurons were sequentially imaged at 40× using red and green fluorescent cubes (Semrock, Inc., Rochester, NY, USA). We manually drew a line down the length of the longest dendrite on the green fluorescent image and then used the linear profile algorithm to measure both red fluorescent channel signal and GFP fluorescence along the dendrite. The line was set to a width of 1 μm. Background fluorescence was measured for each image and subtracted from the linear profile data in Excel. Measurements and analysis were performed by an experimenter who was blinded to the channel variant being tested.

Measuring dendritic arborization

Hippocampal neurons cultured 1 DIV were transfected with plasmids encoding mCherry under the control of the synapsin-1 promoter and untagged $Ca_v3.2$-containing plasmids. Cultures were incubated with indicated drugs from the following day and replenished daily. Cells were fixed with paraformaldehyde and red fluorescence was imaged as described above. The total size of the neuron was estimated using the autosegment function of IPLab software. Images were converted to a TIF format and traced in Neurolucida (MBF Bioscience, Inc., Williston, VT, USA) using the Autoneuron function, followed by manual editing if necessary, and subjected to node analysis and Scholl analysis of arborization.

Transactivator trap luciferase assay

Mature cultured neurons (7–8 DIV) were transfected as described above with the following plasmids: untagged Syn-mGFP-2A-$Ca_v3.2$-WT or C456S; pGL4.35 (luc2P-9XGAL4-UAS; Promega Corp., Fitchburg, WI, USA), and Gal4-Crest (Aizawa *et al.* 2004). One day after transfection, the medium was supplemented with KCl to achieve a final concentration of 10 mM and, as noted, TTA-P2 was added to a final concentration of 300 nM. Cells were harvested 1 day later and luciferase activity was measured following the manufacturer's directions (Luciferase Assay System; Promega Corp.) using a Lumat 9507 luminometer (Berthold Technologies GmbH, Bad Wildbad, Germany).

Results

Expression of C456S mutant increases excitability of hippocampal neurons

In our previous studies, we demonstrated that mutations detected in $Ca_v3.2$ T-type calcium channels in patients with CAE (Chen *et al.* 2003) substantially modify the biophysical properties and surface expression level of the recombinant $Ca_v3.2$ channels in HEK-293 cells (Vitko *et al.* 2005, 2007). Computer modelling led us to the hypothesis that increased seizure susceptibility in CAE patients might be caused by increased T-currents leading to increased spontaneous activity of neurons in the epileptic circuit (Vitko *et al.* 2005). To test this hypothesis directly, we transfected cultured hippocampal neurons with plasmids encoding WT $Ca_v3.2$ and the CAE variant C456S, and then studied spontaneous activity. To unambiguously identify neurons expressing these channels, we engineered a bicistronic construct

that simultaneously drives expression of the T-channels and mCherry (Supplemental Fig. 1*A*). This ensured that recording from red fluorescent neurons would accurately record the effect of recombinant T-channels. Recording fluorescent cells using whole-cell patch-clamp configuration in current-clamp mode, we observed clear differences in the firing patterns of these two groups (Fig. 1*A*). Neurons showed typical epileptiform firing patterns such as burst firing and paroxysmal depolarizing shifts. Because whole-cell current-clamp mode leads to dialysis of the intracellular solution and alterations in both resting membrane potential (V_m), and AP firing, we switched to the loose cell-attached patch method, which can measure firing without such artefacts (Nunemaker *et al.* 2003). Mature cultures of hippocampal neurons form extensive synaptic contacts; therefore, to isolate intrinsic spontaneous activity the extracellular solution was supplemented with blockers of synaptic transmission (see Methods). In addition, we reduced extracellular Mg^{2+} to 0.6 mM to increase firing activity (Mody *et al.* 1987). Spontaneous APs were observed in 90% of neurons expressing C456S and in 60% of neurons expressing WT channels. Additionally, the frequency of spontaneous APs detected in neurons expressing C456S was significantly higher than that detected in neurons expressing WT channels (Fig. 1*C*). As a transfection control, we developed a non-conducting variant of $Ca_v3.2$ using a strategy similar to that used in $Ca_v1.2$ (Dirksen & Beam 1999), replacing a key aspartate residue in the pore with lysine (D1504K). Preliminary recordings in transfected HEK-293 cells confirmed the absence of ionic currents from this mutant (Supplemental Fig. 2). Spontaneous firing in neurons expressing D1540K was significantly lower than in those expressing C456S ($P < 0.001$). We also analysed the inter-spike interval (ISI) in this spontaneous firing data (Fig. 1*D*). This analysis revealed that over half of the APs in neurons transfected with C456S occurred in <100 ms, the duration of a typical LTS (Perez-Reyes,

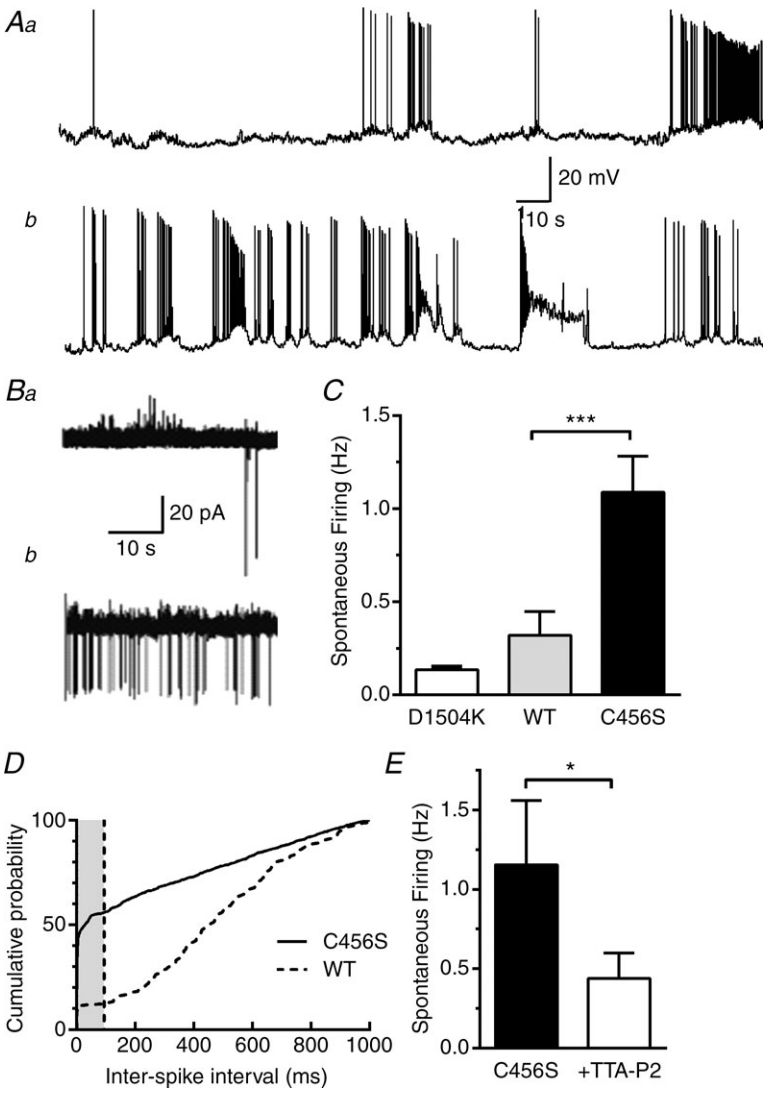

Figure 1. C456S increases spontaneous activity of hippocampal neurons
A, spontaneous firing of neurons expressing either wild-type (WT) (*Aa*) or C456S (*Ab*) channels recorded in the whole-cell current-clamp mode. To measure spontaneous firing without cell dialysis, we used the loose cell-attached patch recording mode. *B*, representative traces of spontaneous activity measured from neurons transfected with either WT (*Ba*) or C456S (*Bb*). Scale bars are shown at the ends of traces *Aa* and *Ba*. *C*, average spontaneous firing recorded in loose cell-attached patch configuration ($n = 15$ or 16). The Mann–Whitney test was used for statistical analysis. ***Significance at $P < 0.001$. A non-conducting mutant, D1504K, was used as a transfection control ($n = 6$). *D*, the time interval between action potentials (APs) was calculated and expressed as the cumulative probability. The grey shaded area corresponds to APs that were separated by <100 ms. *E*, the selective T-type Ca^{2+} channel blocker TTA-P2 (1 μM) blocked spontaneous firing by 66% (C456S 1.2 ± 0.4 Hz, TTA-P2 0.4 ± 0.2 Hz; $n = 6$, $P < 0.05$) and significantly increased the median inter-spike interval from 5 ms to 29 ms (95% confidence intervals: C456S, 3–8; plus TTA-P2, 27–31).

Table 1. Electrophysiological properties of cultured hippocampal neurons in whole-cell recordings

	Untransfected	Wild-type	C456S
Current clamp			
Resting membrane potential (mV)	−61 ± 3	−62 ± 2	−64 ± 2
Input resistance (GΩ)	0.33 ± 0.04	0.49 ± 0.05*	0.47 ± 0.03
Number of cells	12	19	15
Voltage clamp			
Capacitance (MΩ)	151 ± 23	143 ± 11	125 ± 12
Peak current −50 mV (pA)	−98 ± 25	−495 ± 83†	−811 ± 99*
Number of cells	6	13	11

Statistical significance was calculated for comparisons between either untransfected and wild-type or wild-type and C456S (Mann–Whitney test: $^*P < 0.05$; $\dagger P < 0.01$). Differences in V_m and capacitance were not statistically significant.

2003). In contrast, only ∼10% of WT APs occurred at these frequencies. These results suggest that C456S channels increased burst firing at the resting membrane potential of cultured hippocampal neurons (approximately −60 mV; Table 1). To confirm the pacemaker role of T-channels in this spontaneous firing, we tested the ability of the selective T-channel blocker TTA-P2 (Dreyfus *et al.* 2010). Preliminary data using recombinant WT $Ca_v3.2$ channels showed this concentration (1 μM) blocked >95% of the T-current (Supplemental Fig. 3). TTA-P2 blocked spontaneous firing in C456S transfected cells by ∼66% and increased the median ISI from 5 ms to 29 ms (Fig. 1*E*). These results confirm our original hypothesis that neurons expressing a CAE variant found in *CACNA1H* have increased excitability.

C456S channels influence neuronal excitability by reducing the threshold for LTS generation

To investigate mechanisms responsible for the increased excitability of neurons expressing C456S channels, we investigated the electrophysiological properties of transfected cells that might affect their excitability. We first investigated the resting properties of cultured hippocampal neurons. We found that neurons expressing C456S and WT $Ca_v3.2$ channels have similar resting membrane potentials and input resistances (Table 1). A prominent feature of T-channels is the ability to generate rebound bursts of APs after hyperpolarization of the cell by inhibitory postsynaptic potentials (Cheong & Shin 2013). Therefore, we next investigated this property in cultured hippocampal neurons expressing T-channels. To measure rebound APs, neurons were transiently hyperpolarized to −80 mV by negative current injections and then allowed to return to the resting membrane potential. As this failed to elicit rebound firing, we followed the hyperpolarizing step with a series of depolarizing steps (Fig. 2*A*, inset). These small depolarizations elicited classical low-threshold Ca^{2+} spikes crowned by one or two Na^+ channel-mediated APs (Llinás & Jahnsen 1982). Neurons transfected with C456S showed larger LTS depolarizations than WT at all membrane potentials achieved by the depolarizing current injection (Fig. 2*B*). Correspondingly, the amount of current (pA) required to trigger APs, or rheobase, was considerably lower in neurons expressing C456S than in neurons expressing WT channels or untransfected neurons (Fig. 2*C*). In addition, the latency to the first AP measured in C456S-expressing neurons was significantly shorter (Fig. 2*C*). A hallmark of burst firing after T-channel mediated LTS is the presence of an after-depolarizing potential (ADP) (Su *et al.* 2002). Closer examination of current traces recorded during the protocol shown in Fig. 1*A* revealed the ADP. Neurons transfected with C456S showed significantly larger and longer-lasting ADPs than WT transfected neurons after small depolarizations, but not after larger depolarizations when the LTS amplitude began to converge (Fig. 1*F*). These results suggest that the C456S epilepsy mutation in $Ca_v3.2$ channels can affect neuronal excitability by reducing the threshold for LTS generation.

Increased T-current was detected in neurons expressing C456S channels

Our previous studies showed that some CAE variants affected the biophysical properties of $Ca_v3.2$ channels in a manner that would increase activity (Vitko *et al.* 2005). Notably, all variants increased cell surface expression of $Ca_v3.2$ channels in HEK-293 cells, albeit modestly (25–50% above WT) (Vitko *et al.* 2007). For these studies, we selected the C456S mutant for the following reasons: it increased surface expression by 50%; it shifted the current–voltage (*I–V*) curve 5 mV to more hyperpolarized potentials with no effect on the voltage dependence of inactivation, thereby opening the window current range, and it had a dramatic effect on predicted firing in the NEURON model (Vitko *et al.* 2005, 2007). To test the expression level of C456S channels in cultured

hippocampal neurons, we first measured the amplitude of calcium currents in transfected and untransfected neurons using whole-cell voltage-clamp configuration. As expected from their low-voltage activation, voltage-clamping neurons to −50 mV elicited almost exclusively transient LVA T-currents (Fig. 3*A*, *B*). To isolate high voltage-activated (HVA) currents, we held the neurons at a voltage at which T-channels were inactive (Fig. 3*C*) and elicited currents with depolarizing pulses. Similar to the traces shown in Fig. 3*A*, these currents showed only 35% inactivation during a 100 ms pulse. The resulting *I–V* curves are typical of LVA and HVA channels, showing a 23 mV difference in the voltage of half activation (Perez-Reyes, 2003). Similarly, the activation and inactivation kinetics of these currents matched previous studies of endogenous T-currents in hippocampal

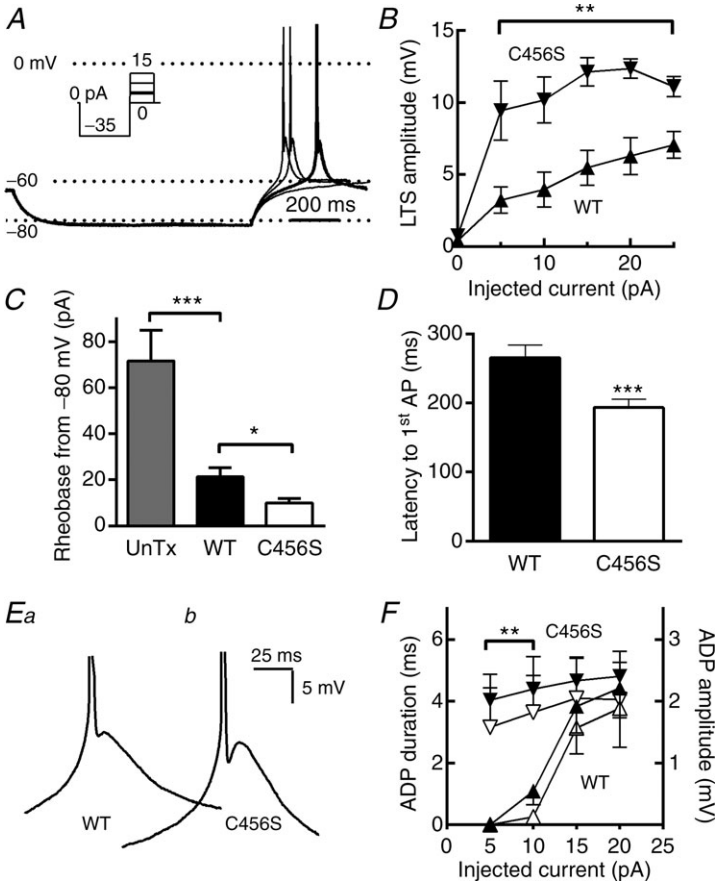

Figure 2. C456S increases low-threshold depolarization leading to faster action potential (AP) generation and larger after-depolarizations
A, representative current-clamp traces from four consecutive sweeps. This cell was at the typical resting membrane potential of −60 mV (V_m). Injection of –35 pA current hyperpolarized the membrane to −82 mV. After this hyperpolarizing current injection, the neuron was allowed to return to the resting membrane potential or injected with small depolarizing current pulses. In this example, injection of 5 pA current triggered a low-threshold spike that was crowned with an AP (bold trace). *B*, the amplitude of the low-threshold depolarization was estimated from the peak of the after-depolarization to the baseline V_m, and plotted as a function of the depolarizing current amplitude. *C*, quantification of the amount of depolarizing current (pA) required to trigger an AP (rheobase) when cells were hyperpolarized to −80 ± 1 mV. *D*, average latency from the end of the hyperpolarizing pulse to the AP. *E*, representative low-threshold spikes from neurons transfected with either wild-type (WT) (*Ea*) or C456S (*Eb*) are shown at an expanded scale to highlight the after-depolarizing potential (ADP). *F*, quantification and statistical analysis of the ADP. ADP durations and amplitudes were estimated from the trough after the AP to the ADP peak. Average ADP durations are shown in solid triangles and amplitudes in open triangles. In all figures WT data are represented with upward triangles (▲) and C456S with downward triangles (▼). Student's *t* test was used for statistical analysis (*B*, *F*); the Mann–Whitney test was used for analysis of other data (*C*, *D*). $^*P < 0.05$; $^{**}P < 0.01$; $^{***}P < 0.001$. Data were recorded from: (1) untransfected neurons ($n = 12$); (2) neurons transfected with a plasmid encoding WT $Ca_v3.2$ channels ($n = 19$), or (3) neurons transfected with a plasmid encoding the childhood absence epilepsy variant of $Ca_v3.2$, C456S ($n = 17$).

neurons (Toselli & Taglietti 1992), as well as work with recombinant Ca_v3 channels (Perez-Reyes, 2003). We used the transient property to the T-current to compensate for a small (6–10%) amount of HVA current measured at −50 mV, then divided by the cell capacitance (Table 1). T-currents of significantly greater amplitude were detected in neurons expressing C456S channels than in WT $Ca_v3.2$-expressing or untransfected neurons (Fig. 3*D*). Together these results suggest that C456S mutants increase neuronal excitability and lower the threshold for LTS generation by increasing T-current.

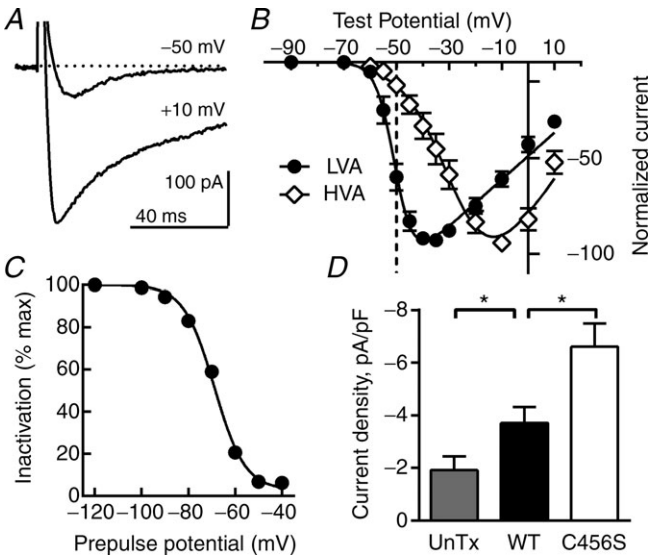

Figure 3. Expression of $Ca_v3.2$ in cultured hippocampal neurons increases T-type currents
A, representative current traces recorded in whole-cell voltage-clamp from a neuron transfected with a plasmid encoding $Ca_v3.2$ channels with the C456S mutation. From a holding potential of –80 mV, a test pulse to –50 mV elicits a low-threshold, transient [low-voltage activated (LVA)] current. Further depolarization to +10 mV elicits slower inactivating currents. *B*, T-currents were estimated from *I–V* protocols (Hp = −90 mv) by exploiting their transient kinetics; the current at the end of the 100 ms depolarizing pulse was subtracted from the peak current and then averaged (LVA). High voltage-activated (HVA) currents were measured in isolation after inactivating LVA currents by holding the cell at –65 mV. Smooth curves are fits to the average data with a Boltzmann–Ohm equation (Gomora *et al.* 2002): LVA $V_{0.5} = -50.4 \pm 0.4$, $k = 3.5 \pm 0.4$, $n = 22$; HVA, $V_{0.5} = -27.3 \pm 1.5$, $k = 8.7 \pm 0.9$, $n = 10$). *C*, steady-state inactivation properties of the LVA currents estimated with 1 s prepulses followed by a test pulse to –40 mV to measure channel availability. A smooth curve represents a fit to the average data with a Boltzmann equation: $V_{0.5} = -68.8 \pm 0.5$, $k = -6.5 \pm 0.4$ ($n = 25$). *D*, average current amplitude normalized to cell capacitance from: (1) untransfected neurons ($n = 6$); (2) neurons transfected with a plasmid encoding wild-type (WT) $Ca_v3.2$ channels ($n = 13$), or (3) neurons transfected with a plasmid encoding the childhood absence epilepsy variant of $Ca_v3.2$, C456S ($n = 11$). The Mann–Whitney test was used for statistical analysis. $^*P < 0.05$.

Trafficking of $Ca_v3.2$ channels and variants in hippocampal neurons

To study $Ca_v3.2$ channel trafficking, we developed a novel plasmid vector that expressed HA-tagged channels and used a 2A-peptide bridge to express GFP (Supplemental Fig. 1*B*). Despite its usefulness for identifying transfected neurons, the bicistronic vector used in the electrophysiology studies did not produce enough mCherry signal to visualize the entire neuron. As there are no commercially available antibodies that recognize extracellular epitopes, and hence channels at the PM, we used HA-tagged channels. Bourinet and co-workers placed the small HA epitope (YPYDVPDYA) in the extracellular facing loop between repeat I S3 and S4 segments (Dubel *et al.* 2004). Notably, this addition does not affect channel function and has proven useful for studying how CAE variants affect trafficking in HEK-293 cells (Vitko *et al.* 2007). Because trafficking of mRNA in neurons often involves motifs in the 3′ untranslated region (UTR) (Raab-Graham *et al.* 2006), we PCR cloned and ligated the full 782 bp UTR. This plasmid was transfected into mature hippocampal neurons and then studied 1 week later to allow for expression and trafficking. To prevent staining of intracellular channels, we stained live neurons with a monoclonal HA-antibody. Neurons were then fixed with paraformaldehyde and stained with the 2° antibody, a goat anti-mouse antibody coupled to Alexa Fluor 568, then mounted on slides for microscopy. Imaging of both red and green fluorescent signals was performed on neurons with either pyramid- or stellate-shaped cell bodies, focusing on the longest dendrite. Representative images are shown in Fig. 4*A*. The GFP signal was brightest at the cell body, then decayed monotonically down the length of the dendrite (Supplemental Fig. 4). In contrast, the red fluorescent signal of HA-tagged channels remained uniform. We calculated the ratio of the two signals for the following reasons: (1) to normalize for varying transfection efficiencies; (2) to normalize for the amount of plasmid taken up by each neuron, and (3) to normalize for the decreasing width of the dendrite as it extends from the cell body. As shown in Fig. 4*B*, the HA : GFP ratio increased over the first 100 μm from the cell body. Deletions in the intracellular loop that separates repeat I and II led to large increases in the amount of channel at the PM (Fig. 4*C*; location of deletions and epilepsy mutations shown in Supplemental Fig. 5). An exception was the D1 deletion, which deletes the most proximal part of the loop. Although the effect of C456S in increasing T-currents was statistically significant, its effect on trafficking was not. The I–II loop contains many RxR and Yxxϕ motifs that may play a role in channel trafficking to and from the PM (Boll *et al.* 1996; Shikano & Li 2003). As the D2 deletion removes one of these Yxxϕ motifs (YARW) and increases cell surface expression, we mutated this motif to

AARA (Y479A, R481A and W482A). This mutation did increase surface expression of $Ca_v3.2$, but not to the same extent as the D2 deletion. Unlike D2, which induces large shifts in the voltage dependence of gating (Vitko *et al.* 2007), the AARA mutation had little effect on channel biophysics (Supplemental Fig. 6). The results in Fig. 4*B* suggest that $Ca_v3.2$ channels are preferentially trafficked into dendrites. To test whether motifs in the I–II loop were responsible for this effect, we re-plotted the data to the maximum HA : GFP ratio observed. These curves were superimposable (Fig. 4*D*). We also measured trafficking of channels down the longest dendrite and found no difference between the variants (Fig. 4*E*).

The CAE mutant C456S enhances growth and dendritic arborization

Freshly isolated hippocampal neurons from E18 pups differentiate rapidly in culture, attaining dendritic trees after 3–4 days (Kaech & Banker 2006). As Ca^{2+}-activated transcription factors such as CREST have been shown to increase dendritic arborization of cultured neurons

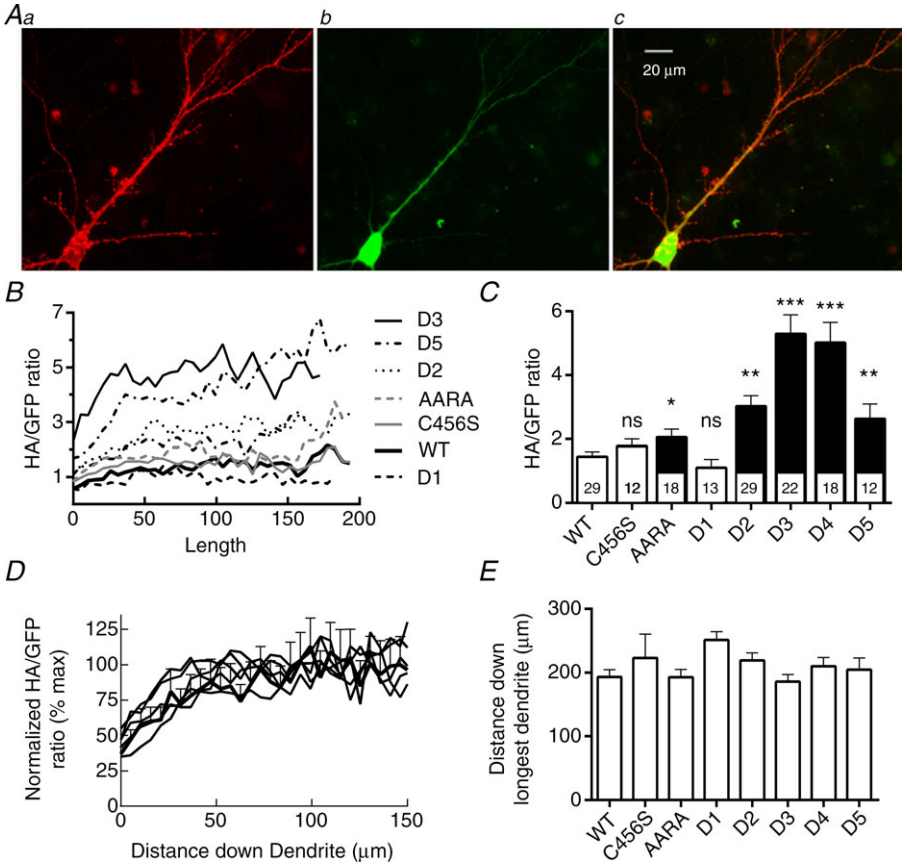

Figure 4. $Ca_v3.2$ channel variants demonstrate increased trafficking to the surface of hippocampal neurons
A, images of a single neuron transfected with the plasmid Syn-mGFP-2A-$Ca_v3.2$-D4. *Aa*, surface channels were labelled with a mouse anti-HA monoclonal primary antibody and a goat anti-mouse Alexa Fluor 568 secondary antibody. *Ab*, green fluorescent protein (GFP) fluorescence was imaged without immunofluorescent amplification. *Ac*, merge of the two previous images. *B–D*, analysis of channel and GFP trafficking from the soma down the length of the longest dendrite. All images of a particular fluorophore were acquired with exposures of the same duration to allow for comparison. *B*, the ratio of the HA-tagged channel signal to the GFP signal is plotted as a function of distance away from the cell body. The ratio for each cell was calculated, then averaged. Error bars are not shown for clarity. *C*, the maximal HA : GFP ratio was calculated as the average signal observed between 100 μm and 150 μm from the cell body, where the signal plateaus (see *D*). ANOVA was used for statistical analysis; numbers of cells studied are shown inside the respective column in *C*. Significant differences from wild-type (WT) $Ca_v3.2$ channels are indicated as follows: $^*P < 0.05$; $^{**}P < 0.01$, and $^{***}P < 0.001$. *D*, the data in panel *B* were normalized to the maximum ratio observed (indicated as %) and plotted as a function of distance down the dendrite. Error bars are shown for WT channels to emphasize that there were no statistical differences between the curves. *E*, the distance from the soma that the channel trafficked down the longest dendrite. Measurement ended when the HA-signal was <2 standard deviations above the background signal. There was no statistical difference between the channel variants.

(Aizawa *et al.* 2004), we tested the hypothesis that increased T-currents might activate the same pathway. We transfected neurons with plasmids 24 h after isolation and allowed them to grow for a further 3 days. Neurons were then fixed, imaged and analysed using Neurolucida software. To block T-current-mediated effects, we included the absence epilepsy drug ethosuximide (ESX) at a clinically relevant concentration, 0.3 mM (Fig. 5*A*, *B*) or the investigational T-channel blocker TTA-P2 at 0.3 μM (Dreyfus *et al.* 2010). We also used the D1504K non-conducting $Ca_v3.2$ mutant as a transfection control. Representative images of neurons expressing C456S in the absence and presence of ESX are presented in Fig. 5*A*. Average results show that ESX reduced the growth in total neuron size induced by C456S to the value observed with the non-conducting mutant (Fig. 5*B*). Scholl analysis revealed that C456S also increased the total number of nodes (Fig. 5*C*) and arborization (Fig. 5*D*) relative to the D1504K mutant. Again, TTA-P2 blocked the effect of C456S. We also tested the effect of TTA-P2 on the transfection control and found no effect (Fig. 5*C*).

The Ca^{2+}-activated transcription factor CREST was discovered using a Gal4 transactivator trap assay (Aizawa *et al.* 2004). We obtained the plasmids and replaced the chloramphenicol acetyltransferase reporter with the destabilized luciferase reporter Luc2 (Promega Corp.). Mature neurons were transfected with the transactivator trap plasmids plus either WT $Ca_v3.2$ or C456S variant. To enhance LVA Ca^{2+} channel activity, we depolarized neurons with 10 mM KCl, which according to the Nernst equation should bring the membrane to −48 mV. After 1 day of incubation, neurons were lysed and luciferase activity was measured using luminometry. Neurons transfected with C456S had higher luciferase activity than

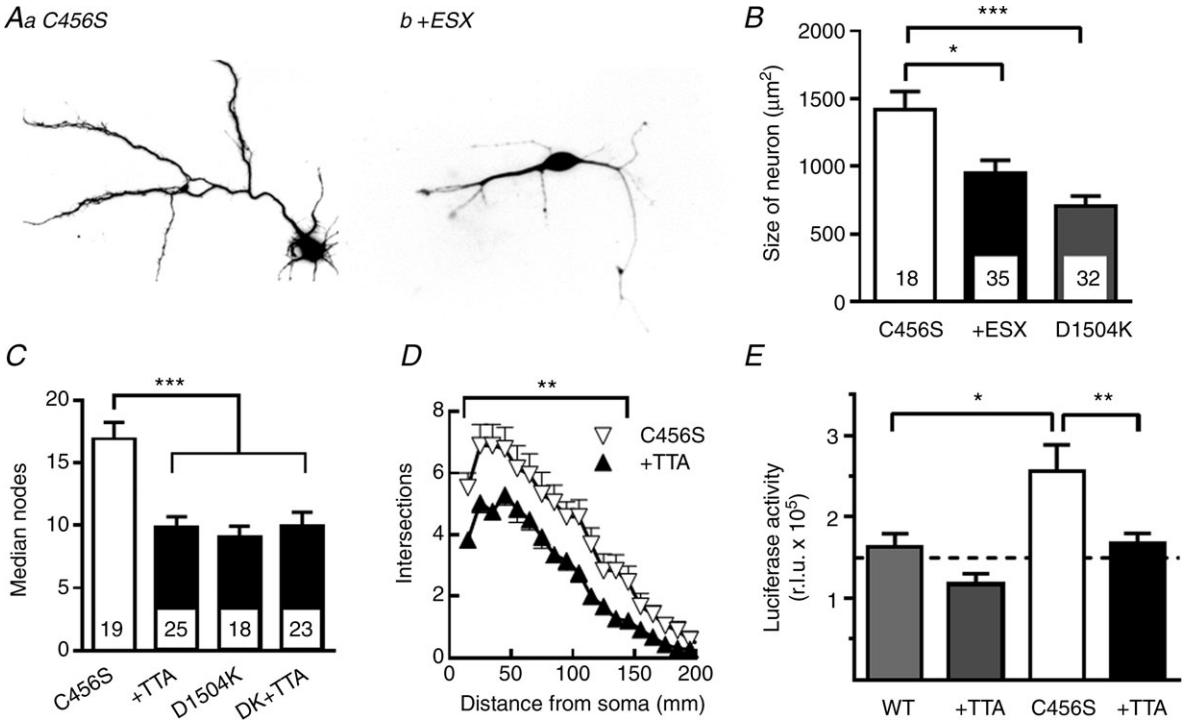

Figure 5. $Ca_v3.2$ channel mutants increased differentiation of immature hippocampal neurons
A, representative images of neurons transfected with plasmids encoding mCherry and the childhood absence epilepsy variant C456S. The cells were transfected 1 day after isolation from E19 embryonic hippocampal tissue. The neurons were maintained in Neurobasal medium in the absence (*Aa*) and presence (*Ab*) of 0.3 mM ethosuximide (ESX) for 3 days before imaging. *B–D*, cells were analysed with Neurolucida software to determine their overall size (*B*), number of branch points (*C*) and Scholl analysis of dendritic arborization (*D*). D1504K is a non-conducting $Ca_v3.2$ channel variant that was used as transfection control (Supplemental Fig. 2). The data in panels *C* and *D* are from separate experiments in which the selective T-type channel antagonist, TTA-P2 (0.1 μM TTA), was used instead of ESX. *E*, the Gal4-transactivator trap system (Aizawa *et al.* 2004) was used to measure T-channel signalling to the Ca^{2+}-activated transcription factor CREST. Hippocampal neurons were transfected with the plasmids pGL4.35, Gal4-Crest, and Syn-mGFP-2A-$Ca_v3.2$-WT or C456S, and harvested 48 h later for luciferase assay. Results refer to a representative experiment performed four times, in which statistical differences were calculated with Student's *t* test. The addition of TTA-P2 had no statistical effect on the luciferase activity measured in cells transfected with wild-type channels, but reversed the effect of C456S channels ($n = 6$ replicates). ANOVA was used for statistical analysis. Numbers of cells studied are shown inside the respective columns (*B*, *C*). Significant differences from C456S channels are shown: $^*P < 0.05$; $^{**}P < 0.01$, and $^{***}P < 0.001$.

those transfected with WT, and this effect was blocked by TTA-P2 (Fig. 5*E*).

Discussion

The goal of these studies was to investigate the mechanisms by which epilepsy mutations in the gene that encodes $Ca_v3.2$, *CACNA1H*, might increase seizure susceptibility. We first demonstrated that expression of C456S channels significantly increases the excitability of cultured hippocampal neurons. This result validates computer modelling studies based on the biophysical properties of WT and C456S channels (Vitko *et al.* 2005; Xu & Clancy 2008). C456S was also found to increase rebound LTSs that triggered APs. The C456S variation also increased T-current density, consistent with increased trafficking to the neuronal PM as predicted by studies in HEK-293 cells (Vitko *et al.* 2007). Our trafficking studies showed the important role played by the I–II loop in $Ca_v3.2$ expression in neurons. Notably, by studying the role of a known trafficking motif, we can begin to understand why almost all CAE mutations or deletions in the I–II loop increase trafficking to the neuronal surface. The final key result was to show that an epilepsy variant increased the activity of the Ca^{2+}-regulated transcription factor CREST. In combination with the well-described role of activity-modulated gene expression (West & Greenberg 2011), this result suggests that a *CACNA1H* variant can activate widespread changes in gene expression. Blockage of the variant Ca^{2+} current by either ESX or TTA-P2 returned neuronal development to baseline, as assessed with the non-conducting D1504K mutant. This suggests that endogenous $Ca_v3.2$ channels have a limited role in normal dendritic development, and that T-channel-blocking drugs will not retard development. This point warrants further study as loss-of-function mutations in *CACNA1H* have been linked to disorders on the autism spectrum (Splawski *et al.* 2006).

In lay terms, epilepsy is a disorder in which the balance between excitatory and inhibitory neurotransmission is tipped towards excitability. Therefore, we can predict that T-channel variants that cause the following changes in gating could increase seizure susceptibility: (1) a shift of the voltage-dependence of activation to more negative potentials; (2) a shift of the voltage dependence of inactivation to less negative potentials; (3) acceleration of channel opening; (4) slowing of channel inactivation; (5) slowing of deactivation (open to close transitions); (6) acceleration of recovery from inactivation; (7) an increase in the probability of channel opening (P_o), and (8) an increase in single-channel conductance. Notably, variants associated with IGE do affect many of these properties (Vitko *et al.* 2005), a finding that has been replicated by Zamponi and colleagues (Khosravani & Zamponi 2006; Heron *et al.* 2007). Computer modelling suggested that some of the changes induced by epilepsy variants would lead to a gain of function and increase neuronal firing activity (Vitko *et al.* 2005; Xu & Clancy 2008). The present study directly tested this hypothesis and found that the C456S variant led to hyperactive neurons with enhanced rebound LTSs.

Idiopathic generalized epilepsies are thought to arise from increased activity of the thalamocortical loop (Crunelli & Leresche 2002). Thalamic neurons express some of the highest T-current densities observed in electrophysiological studies (Perez-Reyes, 2003). Interestingly, rodent *CACNA1H* is highly expressed in the reticular nucleus of the thalamus, and its expression is increased in the GAERS rat, which represents a model of absence epilepsy (Talley *et al.* 1999, 2000). In fact, a mutation in *CACNA1H* was found in the GAERS rat and shown to increase seizure susceptibility in a polygenic manner (Powell *et al.* 2009). Therefore, the results of the present study suggest that gain-of-function *CACNA1H* mutations would be likely to alter firing and gene expression in thalamocortical networks to increase seizure susceptibility. Initial attempts to culture thalamic neurons were hampered by de-differentiation and loss of T-currents (A. Shcheglovitov, unpublished observations, 2004). In contrast, an extensive body of literature supports the utility and proper development of cultured hippocampal neurons (Kaech & Banker 2006). A role for $Ca_v3.2$ upregulation in hippocampal neurons has also been reported in animal models of TLE, leading to increased ADPs, spontaneous activity, and burst firing of hippocampal neurons (Su *et al.* 2002). Transgenic mice lacking $Ca_v3.2$ expression are resistant to developing spontaneous seizures in the pilocarpine model of TLE (Becker *et al.* 2008). $Ca_v3.2$ upregulation and increased burst firing of midline thalamic neurons have also been observed in a mouse model of TLE (Graef *et al.* 2009). Human TLE is provoked by damage such as fever, traumatic brain injury or *status epilepticus*. Recent studies have uncovered a genetic predisposition for TLE (Tsai *et al.* 2013), suggesting that seizure susceptibility genes such as *CACNA1H* may be involved in many forms of epilepsy.

Our studies have focused on the original set of variants discovered in Chinese CAE patients (Chen *et al.* 2003). Although these specific variants have not been identified in other populations (Chioza *et al.* 2006), other variants have been found to be associated with the larger classification of IGEs (Heron *et al.* 2004, 2007). Again, many sequence variants in *CACNA1H* were discovered in a large screen of ion channel gene variants in patients with idiopathic epilepsy (Klassen *et al.* 2011). It is interesting to note that six of the eight variants detected in this Baylor Ion Channel Project were located in the I–II loop (A555V, V664A, P701L, E718G, G755D and T947I; locations shown in Supplemental Fig. 5). Our previous studies, and those by others, found the original

Chinese CAE variants produced subtle effects on the biophysical properties of $Ca_v3.2$ channels (Khosravani *et al.* 2004; Vitko *et al.* 2005). Accordingly, NEURON modelling of these biophysical effects revealed that only five of the 13 variants studied increased predicted firing (Vitko *et al.* 2005). This result seemingly contradicted the hypothesis that all $Ca_v3.2$ variants increased susceptibility to IGEs. This conundrum was partially resolved by a study on their effect on channel trafficking to the PM using a plate assay of millions of HEK-293 cells, which showed that variants that failed to increase firing did increase surface expression (Vitko *et al.* 2007). Mechanisms by which this might occur include: (1) enhanced trafficking out of endoplasmic reticulum/Golgi to PM; (2) slower retrieval from the PM; (3) an altered fate of internalized early endosomes from degradation to PM recycling, and (4) altered distribution of T-channels in neurons (e.g. enhanced trafficking into dendrites, or increased expression at the axon hillock). The I–II loop of Ca_v3 channels shows two areas of conservation separated by mostly non-conserved sequence. The proximal loop contains a highly conserved region that restrains T-channel opening near the resting membrane potential (Arias-Olguín *et al.* 2008). Consistent with its lack of conservation, the I–II loop plays distinct roles amongst the Ca_v3 channel family (Baumgart *et al.* 2008), with a dominant inhibitory role in $Ca_v3.2$, a modest inhibitory role in $Ca_v3.1$, and a forward trafficking role in $Ca_v3.3$ channels. Sequence comparisons among the three channels identified non-conserved trafficking motifs, including many RxR and Yxxϕ motifs that are involved in trafficking to and from the PM (Boll *et al.* 1996). Our results show that mutation of just one of the seven Yxxϕ motifs found in the I–II loop is sufficient to increase surface expression. This result suggests mutations might reduce removal from the PM or alter sorting in the endocytic pathway. We conclude that the deletion mutants each result in a similar phenotype because they all delete similar Yxxϕ motifs. As none of the mutations affected trafficking into dendrites, we conclude that the I–II loop is not involved in this process.

Because both the biophysical and trafficking effects were modest, we selected the C456S mutant for the present studies as it was predicted to have the largest effect on neuronal excitability (Vitko *et al.* 2005; Xu & Clancy 2008). During a study aimed at understanding how β subunits regulate HVA Ca^{2+} channels, we accidentally discovered that the I–II loop plays a role in channel expression (Arias *et al.* 2005). Subsequent studies found the existence of a gating brake in the proximal I–II loop that plays an important role in the LVA nature of these channels (Arias-Olguín *et al.* 2008; Karmazinova *et al.* 2011). The C456S mutation lies in the middle of this highly conserved gating brake, providing a mechanistic explanation for its ability to affect channel gating. Our finding that C456S makes neurons hyperactive confirms computer modelling studies of thalamic and hippocampal neurons (Vitko *et al.* 2005; Xu & Clancy 2008). Its ability to modify model firing largely results from its ability to shift the voltage dependence of activation by −5 mV (Vitko *et al.* 2005). However, close examination of the firing patterns shown in Fig. 1 reveal long-lasting bursts and plateau potentials that resemble paroxysmal depolarizing shifts, which require the involvement of other ion channels such as high-threshold Ca^{2+} channels and glutamate-gated channels (Fraser & MacVicar 1996). Our studies show that $Ca_v3.2$ channels can activate Ca^{2+}-regulated transcription factors, which, in turn, regulate a large set of activity-dependent genes (West & Greenberg 2011). We conclude that *CACNA1H* mutations that affect T-current activity will not only affect firing through their pacemaker activity, but will alter the expression of many genes. This mechanism may provide an explanation for how loss-of-function mutations in *CACNA1H* can lead to autism spectrum disorders (Splawski *et al.* 2006). Similarly, changes in gene expression may explain the indirect autocrine pathway by which $Ca_v3.2$ regulates neurite outgrowth in neuroblastoma NG108–15 cell cultures (Chemin *et al.* 2004).

In the present studies, we were unable to detect a statistical increase in trafficking of C456S channels as a result of cell-to-cell variability (although increased current density was detected). Therefore, it would probably be difficult to measure changes in neuronal excitability in all the *CACNA1H* variants found to date. This notion is in keeping with the modest effects predicted for sequence variants of epilepsy susceptibility genes (Tan *et al.* 2004). With this caveat, we conclude that epilepsy variants increase seizure susceptibility by directly influencing neuronal excitability and indirectly by regulating the activity of other genes involved in neuronal firing. Mutations in any of these other genes could then provide the second hit that characterizes the polygenic inheritance of epilepsy (Klassen *et al.* 2011).

References

Aizawa H, Hu SC, Bobb K, Balakrishnan K, Ince G, Gurevich I, Cowan M, Ghosh A (2004). Dendrite development regulated by CREST, a calcium-regulated transcriptional activator. *Science* **303**, 197–202.

Arias-Olguín II, Vitko I, Fortuna M, Baumgart JP, Sokolova S, Shumilin IA, Van Deusen A, Soriano-Garcia M, Gómora Martinez JM, Perez-Reyes E (2008). Characterization of the gating brake in the I–II loop of $Ca_v3.2$ T-type Ca^{2+} channels. *J Biol Chem* **283**, 8136–8144.

Arias JM, Murbartián J, Vitko I, Lee JH, Perez-Reyes E (2005). Transfer of β subunit regulation from high to low voltage-gated Ca^{2+} channels. *FEBS Lett* **579**, 3907–3912.

Baumgart JP, Vitko I, Bidaud I, Kondratskyi A, Lory P, Perez-Reyes E (2008). I–II loop structural determinants in the gating and surface expression of low voltage-activated calcium channels. *PLoS ONE* **3**, e2976.

Becker AJ, Pitsch J, Sochivko D, Opitz T, Staniek M, Chen C-C, Campbell KP, Schoch S, Yaari Y, Beck H (2008). Transcriptional upregulation of $Ca_v3.2$ mediates epileptogenesis in the pilocarpine model of epilepsy. *J Neurosci* **28**, 13341–13353.

Boll W, Ohno H, Songyang Z, Rapoport I, Cantley LC, Bonifacino JS, Kirchhausen T (1996). Sequence requirements for the recognition of tyrosine-based endocytic signals by clathrin AP-2 complexes. *EMBO J* **15**, 5789–5795.

Broicher T, Kanyshkova T, Meuth P, Pape HC, Budde T (2008). Correlation of T-channel coding gene expression, I^T, and the low threshold Ca^{2+} spike in the thalamus of a rat model of absence epilepsy. *Mol Cell Neurosci* **39**, 384–399.

Chemin J, Monteil A, Briquaire C, Richard S, Perez-Reyes E, Nargeot J, Lory P (2000). Overexpression of T-type calcium channels in HEK-293 cells increases intracellular calcium without affecting cellular proliferation. *FEBS Lett* **478**, 166–172.

Chemin J, Nargeot J, Lory P (2004). $Ca_v3.2$ calcium channels control an autocrine mechanism that promotes neuroblastoma cell differentiation. *Neuroreport* **15**, 671–675.

Chen YC, Lu JJ, Pan H, Zhang YH, Wu HS, Xu KM, Liu XY, Jiang YW, Bao ZH, Yao ZJ, Ding KY, Lo WHY, Qiang BQ, Chan P, Shen Y, Wu XR (2003). Association between genetic variation of *CACNA1H* and childhood absence epilepsy. *Ann Neurol* **54**, 239–243.

Cheong E, Shin HS (2013). T-type Ca^{2+} channels in normal and abnormal brain functions. *Physiol Rev* **93**, 961–992.

Chioza B, Everett K, Aschauer H, Brouwer O, Callenbach P, Covanis A, Dulac O, Durner M, Eeg-Olofsson O, Feucht M, Friis M, Heils A, Kjeldsen M, Larsson K, Lehesjoki AE, Nabbout R, Olsson I, Sander T, Sirén A, Robinson R, Rees M, Gardiner RM (2006). Evaluation of *CACNA1H* in European patients with childhood absence epilepsy. *Epilepsy Res* **69**, 177–181.

Coulter DA, Huguenard JR, Prince DA (1989). Characterization of ethosuximide reduction of low-threshold calcium current in thalamic neurons. *Ann Neurol* **25**, 582–593.

Crunelli V, Leresche N (2002). Childhood absence epilepsy: genes, channels, neurons and networks. *Nat Rev Neurosci* **3**, 371–382.

Crunelli V, Toth TI, Cope DW, Blethyn K, Hughes SW (2005). The 'window' T-type calcium current in brain dynamics of different behavioural states. *J Physiol (Lond)* **562**, 121–129.

Dirksen RT, Beam KG (1999). Role of calcium permeation in dihydropyridine receptor function. Insights into channel gating and excitation-contraction coupling. *J Gen Physiol* **114**, 393–403.

Dreyfus FM, Tscherter A, Errington AC, Renger JJ, Shin HS, Uebele VN, Crunelli V, Lambert RC, Leresche N (2010). Selective T-type calcium channel block in thalamic neurons reveals channel redundancy and physiological impact of I_T window. *J Neurosci* **30**, 99–109.

Dubel SJ, Altier C, Chaumont S, Lory P, Bourinet E, Nargeot J (2004). Plasma membrane expression of T-type calcium channel $\alpha 1$ subunits is modulated by HVA auxiliary subunits. *J Biol Chem* **279**, 29263–29269.

Fraser DD, MacVicar BA (1996). Cholinergic-dependent plateau potential in hippocampal CA1 pyramidal neurons. *J Neurosci* **16**, 4113–4128.

Gargus JJ (2003). Unraveling monogenic channelopathies and their implications for complex polygenic disease. *Am J Hum Genet* **72**, 785–803.

Gomora JC, Daud AN, Weiergräber M, Perez-Reyes E (2001). Block of cloned human T-type calcium channels by succinimide antiepileptic drugs. *Mol Pharmacol* **60**, 1121–1132.

Gomora JC, Murbartián J, Arias JM, Lee J-H, Perez-Reyes E (2002). Cloning and expression of the human T-type channel $Ca_v3.3$: insights into prepulse facilitation. *Biophys J* **83**, 229–241.

Graef JD, Nordskog BK, Wiggins WF, Godwin DW (2009). An acquired channelopathy involving thalamic T-type Ca^{2+} channels after status epilepticus. *J Neurosci* **29**, 4430–4441.

Heron SE, Khosravani H, Varela D, Bladen C, Williams TC, Newman MR, Scheffer IE, Berkovic SF, Mulley JC, Zamponi GW (2007). Extended spectrum of idiopathic generalized epilepsies associated with *CACNA1H* functional variants. *Ann Neurol* **62**, 560–568.

Heron SE, Phillips HA, Mulley JC, Mazarib A, Neufeld MY, Berkovic SF, Scheffer IE (2004). Genetic variation of *CACNA1H* in idiopathic generalized epilepsy. *Ann Neurol* **55**, 595–596.

Huang Z, Lujan R, Kadurin I, Uebele VN, Renger JJ, Dolphin AC, Shah MM (2011). Presynaptic HCN1 channels regulate $Ca_V3.2$ activity and neurotransmission at select cortical synapses. *Nat Neurosci* **14**, 478–486.

Kaech S, Banker G (2006). Culturing hippocampal neurons. *Nature Protoc* **1**, 2406–2415.

Karmazinova M, Baumgart JP, Perez-Reyes E, Lacinova L (2011). The voltage dependence of gating currents of the neuronal $Ca_v3.3$ channel is determined by the gating brake in the I–II loop. *Pflugers Arch* **461**, 461–468.

Khosravani H, Altier C, Simms B, Hamming KS, Snutch TP, Mezeyova J, McRory JE, Zamponi GW (2004). Gating effects of mutations in the $Ca_v3.2$ T-type calcium channel associated with childhood absence epilepsy. *J Biol Chem* **279**, 9681–9684.

Khosravani H, Zamponi GW (2006). Voltage-gated calcium channels and idiopathic generalized epilepsies. *Physiol Rev* **86**, 941–966.

Klassen T, Davis C, Goldman A, Burgess D, Chen T, Wheeler D, McPherson J, Bourquin T, Lewis L, Villasana D, Morgan M, Muzny D, Gibbs R, Noebels J (2011). Exome sequencing of ion channel genes reveals complex profiles confounding personal risk assessment in epilepsy. *Cell* **145**, 1036–1048.

Llinás R, Jahnsen H (1982). Electrophysiology of mammalian thalamic neurons *in vitro*. *Nature* **297**, 406–408.

Llinás RR (1988). The intrinsic electrophysiological properties of mammalian neurons: insights into central nervous system function. *Science* **242**, 1654–1664.

McCormick DA, Contreras D (2001). On the cellular and network bases of epileptic seizures. *Annu Rev Physiol* **63**, 815–846.

Mody I, Lambert JD, Heinemann U (1987). Low extracellular magnesium induces epileptiform activity and spreading depression in rat hippocampal slices. *J Neurophysiol* **57**, 869–888.

Munsch T, Budde T, Pape HC (1997). Voltage-activated intracellular calcium transients in thalamic relay cells and interneurons. *Neuroreport* **8**, 2411–2418.
Nelson MT, Joksovic PM, Perez-Reyes E, Todorovic SM (2005). The endogenous redox agent L-cysteine induces T-type Ca^{2+} channel-dependent sensitization of a novel subpopulation of rat peripheral nociceptors. *J Neurosci* **25**, 8766–8775.
Nelson MT, Todorovic SM, Perez-Reyes E (2006). The role of T-type calcium channels in epilepsy and pain. *Curr Pharm Des* **12**, 2189–2197.
Nunemaker CS, DeFazio RA, Moenter SM (2003). A targeted extracellular approach for recording long-term firing patterns of excitable cells: a practical guide. *Biol Proced Online* **5**, 53–62.
Perez-Reyes E (2003). Molecular physiology of low-voltage-activated T-type calcium channels. *Physiol Rev* **83**, 117–161.
Powell KL, Cain SM, Ng C, Sirdesai S, David LS, Kyi M, Garcia E, Tyson JR, Reid CA, Bahlo M, Foote SJ, Snutch TP, O'Brien TJ (2009). A $Ca_v3.2$ T-type calcium channel point mutation has splice-variant-specific effects on function and segregates with seizure expression in a polygenic rat model of absence epilepsy. *J Neurosci* **29**, 371–380.
Raab-Graham KF, Haddick PC, Jan YN, Jan LY (2006). Activity- and mTOR-dependent suppression of Kv1.1 channel mRNA translation in dendrites. *Science* **314**, 144–148.
Sander T (1996). The genetics of idiopathic generalized epilepsy: implications for the understanding of its aetiology. *Mol Med Today* **2**, 173–180.
Shikano S, Li M (2003). Membrane receptor trafficking: evidence of proximal and distal zones conferred by two independent endoplasmic reticulum localization signals. *Proc Natl Acad Sci U S A* **100**, 5783–5788.
Splawski I, Yoo DS, Stotz SC, Cherry A, Clapham DE, Keating MT (2006). *CACNA1H* mutations in autism spectrum disorders. *J Biol Chem* **281**, 22085–22091.
Su H, Sochivko D, Becker A, Chen J, Jiang Y, Yaari Y, Beck H (2002). Upregulation of a T-type Ca^{2+} channel causes a long-lasting modification of neuronal firing mode after status epilepticus. *J Neurosci* **22**, 3645–3655.
Talley EM, Cribbs LL, Lee JH, Daud A, Perez-Reyes E, Bayliss DA (1999). Differential distribution of three members of a gene family encoding low voltage-activated (T-type) calcium channels. *J Neurosci* **19**, 1895–1911.
Talley EM, Solórzano G, Depaulis A, Perez-Reyes E, Bayliss DA (2000). Low-voltage-activated calcium channel subunit expression in a genetic model of absence epilepsy in the rat. *Mol Brain Res* **75**, 159–165.
Tan NC, Mulley JC, Berkovic SF (2004). Genetic association studies in epilepsy: 'the truth is out there'. *Epilepsia* **45**, 1429–1442.
Tang W, Ehrlich I, Wolff SB, Michalski AM, Wolfl S, Hasan MT, Lüthi A, Sprengel R (2009). Faithful expression of multiple proteins via 2A-peptide self-processing: a versatile and reliable method for manipulating brain circuits. *J Neurosci* **29**, 8621–8629.
Toselli M, Taglietti V (1992). Kinetic and pharmacological properties of high- and low-threshold calcium channels in primary cultures of rat hippocampal neurons. *Pflugers Arch* **421**, 59–66.
Tsai MH, Pardoe HR, Perchyonok Y, Fitt GJ, Scheffer IE, Jackson GD, Berkovic SF (2013). Etiology of hippocampal sclerosis: evidence for a predisposing familial morphologic anomaly. *Neurology* **81**, 144–149.
Tsakiridou E, Bertollini L, de Curtis M, Avanzini G, Pape HC (1995). Selective increase in T-type calcium conductance of reticular thalamic neurons in a rat model of absence epilepsy. *J Neurosci* **15**, 3110–3117.
Vadlamudi L, Andermann E, Lombroso CT, Schachter SC, Milne RL, Hopper JL, Andermann F, Berkovic SF (2004). Epilepsy in twins: insights from unique historical data of William Lennox. *Neurology* **62**, 1127–1133.
Vitko I, Bidaud I, Arias JM, Mezghrani A, Lory P, Perez-Reyes E (2007). The I–II loop controls plasma membrane expression and gating of $Ca_v3.2$ T-type Ca^{2+} channels: a paradigm for childhood absence epilepsy. *J Neurosci* **27**, 322–330.
Vitko I, Chen Y, Arias JM, Shen Y, Wu XR, Perez-Reyes E (2005). Functional characterization and neuronal modeling of the effects of childhood absence epilepsy variants of *CACNA1H*, a T-type calcium channel. *J Neurosci* **25**, 4844–4855.
West AE, Greenberg ME (2011). Neuronal activity-regulated gene transcription in synapse development and cognitive function. *Cold Spring Harb Perspect Biol* **3**.
Xu J, Clancy CE (2008). Ionic mechanisms of endogenous bursting in CA3 hippocampal pyramidal neurons: a model study. *PLoS ONE* **3**, e2056.
Zhou Q, Godwin DW, O'Malley DM, Adams PR (1997). Visualization of calcium influx through channels that shape the burst and tonic firing modes of thalamic relay cells. *J Neurophysiol* **77**, 2816–2825.

Additional information

Competing interests

None declared.

Author contributions

V.-S.E, A.S. and I.V. are first authors and contributed equally to the manuscript. A.S. and V.-S.E. contributed to the collection and analysis of electrophysiology experiments. I.V., C.C.Y. and B.W. generated materials and conducted the neuronal trafficking experiments. D.D. contributed to the collection and analysis of the trafficking experiments. E.P.-R. contributed to the design of the experiments, analysis, interpretation of data, and the writing of the manuscript. All authors contributed to the revision of the article for accuracy and approved the final version. All experiments were performed at the University of Virginia School of Medicine.

Funding

This work was supported by an American Recovery and Reinvestment Act National Institutes of Health grant (NS067456) awarded to E.P.-R.

Acknowledgements

The authors would like to thank Roman Lazarenko and Maxim Kozhemyakin for electrophysiological advice, and Ruth Stornetta for help with Neurolucida. We also thank Olesya Shcheglovitova and Sarah Renner for technical assistance, and Zofia Lasiecka and Joel Baumgart for preliminary experiments. We thank the following for providing materials: Emannuel Bourinet for the HA-$Ca_v3.2$ cDNA, Roger Tsien for the mCherry cDNA, Michal Fortuna for the synapsin promoter cDNA, Douglas Bayliss for the pGreen Lantern plasmid, and Anirvan Ghosh for the Gal4-Trap plasmids. We thank Victor Uebele (Merck Research Laboratories) for the kind gift of TTA-P2.

Authors' present addresses

V.-S. Eckle: Department of Anaesthesiology and Intensive Care, Eberhard-Karls-University, Tübingen, Germany.

A. Shcheglovitov: Department of Neurobiology, Stanford University School of Medicine, Stanford, CA, USA.